Formation of Branched Ruthenium Nanoparticles for Improved Electrocatalysis of Oxygen Evolution Reaction

Watt, John Daniel
Poerwoprajitno, Agus R.
Gloag, Lucy
Benedetti, Tania M.
Cheong, Soshan
Huber, Dale L.
Gooding, Justin J.
Tilley, Richard D.

To be published in: Small

DOI to publisher's version: 10.1002/smll.201804577

DOI: 10.1002/((please add manuscript number))

Article type: Communication

Formation of Branched Ruthenium Nanoparticles for Improved Electrocatalysis of Oxygen Evolution Reaction

*Agus R. Poerwoprajitno, Lucy Gloag, Tania M. Benedetti, Soshan Cheong, John Watt, Dale L. Huber, J. Justin Gooding, and Richard D. Tilley**

A. R. Poerwoprajitno, Dr. L. Gloag, Dr. T. M. Benedetti, Prof. J. J. Gooding, Prof. R. D. Tilley

School of Chemistry, The University of New South Wales, Sydney, NSW 2052, Australia

E-mail: r.tilley@unsw.edu.au

A. R. Poerwoprajitno, Dr. L. Gloag, Dr. T. M. Benedetti, Prof. J. J. Gooding, Prof. R. D. Tilley

Australian Centre for NanoMedicine, The University of New South Wales, Sydney, NSW 2052, Australia

Dr. S. Cheong, Prof. R. D. Tilley

Electron Microscope Unit, Mark Wainwright Analytical Centre, The University of New South Wales, NSW 2052, Australia

Dr. J. Watt, Dr. D. L. Huber

Center for Integrated Nanotechnologies, Sandia National Laboratories, Albuquerque, NM 87185, USA

Keywords: nanoparticles, electrocatalysis, oxygen evolution reaction, crystallinity, ruthenium

Abstract

Branched nanoparticles are one of the most promising nanoparticle catalysts as their branch sizes and surfaces can be tuned to enable both high activity and stability. Understanding how the crystallinity and surface facets of branched nanoparticles affect their catalytic performances is vital for further catalyst development. In this work, we develop a synthesis to form highly branched ruthenium (Ru) nanoparticles with control of crystallinity. We show that faceted Ru branched nanoparticles have improved stability and activity in the oxygen evolution reaction (OER) compared with polycrystalline Ru nanoparticles. This work achieves a low 180 mV overpotential at 10 mA cm^{-2} for hours, demonstrating that record-high stability for Ru nanocrystals can be achieved while retaining high activity for OER. The superior electrocatalytic performance of faceted Ru branched nanoparticles is ascribed to the lower Ru dissolution rate under OER conditions due to low-index facets on the branch surfaces.

Branched and faceted nanoparticles are very attractive for catalytic applications due to their high surface area and controlled surface structure that enable both high activity and stability.[1] To obtain nanoparticles with high activity and stability, the branch structure needs to be precisely controlled synthetically.[1b, 1c] The crystallinity of a material dictates the surface arrangements of atoms and facets that are available at the branches. However, how to modify synthetic methodologies to tune the crystallinity and change the surface structure of nanoparticles has not been widely

studied. Thus, designing new synthetic methods to make metallic nanostructures with control over branching and crystal arrangement of surface atoms is of great importance.

Ru nanoparticles are the most active catalyst for the oxygen evolution reaction (OER) in acid electrolytes, which is the anodic reaction in the water splitting process for H_2 fuel production.[2] Acid electrolytes have the advantage of producing higher current densities than alkaline electrolytes.[3] Oxidized Ru is electrochemically formed on Ru surface above 0.8 V which is the active species for OER.[4] The use of Ru catalysts is limited by the high dissolution rate of high oxidation state Ru species ($Ru^{>4+}$) that form under OER conditions, typically resulting in complete Ru dissolution in the first few cycles.[4,5] Lower dissolution rates have been achieved for single crystal Ru metal surfaces with low index facets[6] and recently, this has been used to produce both stable and active Ru nanoparticles for the first time.[1b] Thus, making low index faceted metal Ru structures to limit the dissolution of Ru nanoparticles is a key target for OER catalysts.

The synthesis of Ru branched nanoparticles with controlled surface facets is challenging.[7] Ru typically adopts a hexagonal close packed (hcp) crystal structure, which has previously produced limited morphologies, with spherical, or unfaceted aggregate polycrystalline nanoparticles typically formed.[8] By using amine surfactants, we have previously shown that Ru hourglass nanoparticles and Au-Ru nanoparticles with low index facets can be successfully synthesized.[1b, 9] There is an

opportunity to use similar amine surfactants in the synthesis of branched Ru nanoparticles to achieve branched and faceted Ru nanocatalysts.

In this work, we have developed a synthetic method to synthesize Ru branched nanoparticles with control of the crystallinity and surface facets. At high ratios of dodecylamine (DDA) surfactant to Ru precursor, polycrystalline Ru nanoparticles form, while low ratios of DDA enable the formation of branches with low index facets exposed (faceted Ru branched nanoparticles). The influence of the surface structure on electrocatalysis is investigated for the OER in acid electrolyte. The faceted Ru nanoparticles were found to have higher activity and prolonged stability when compared to the polycrystalline Ru nanoparticles and that exceed the performance of all Ru and Ir nanocatalysts to date. These improvements could be understood by the much slower dissolution of Ru species from the exposed low index facets during OER. This work demonstrates that synthetically controlling the surface facets can improve both activity and stability of OER catalysts, rather than improving stability at the cost of lower activity.

Branched Ru nanoparticles were synthesized by reducing ruthenium (III) acetylacetonate under H_2 atmosphere using 1-octadecene as the solvent in a Fischer-Porter bottle. The length and crystallinity of the branches was controlled by changing the ratio of DDA, as shown by low resolution TEM images in **Figure 1**a-d. Changing the ratio of DDA to Ru from 5 mol equivalents to 20 mol equivalents resulted in shorter branches. Measured from core to tip, the branch length decreased from 54 ± 10

nm (5 mol equivalents) to 33 ± 8 nm (10 mol equivalents), 18 ± 5 nm (15 mol equivalents) and 13 ± 2 nm (20 mol equivalents), with the width of the branches remaining constant (5.1 ± 0.8 nm, Figure 1). The increase in DDA ratio also resulted in a decrease in crystallinity, as shown by high-resolution TEM (HRTEM) images in Figure 1a-d. The nanoparticles synthesized with 5 mol equivalents and 10 mol equivalents of DDA have single-crystal branches (HRTEM images in Figure 1a-b). A mixed of polycrystalline and crystalline structure was formed by nanoparticles synthesized with 15 mol equivalents of DDA (Figure 1c and S1, Supporting information), and nanoparticles synthesized with 20 mol equivalents of DDA are entirely polycrystalline (Figure 1d). This information is supported by the selected area electron diffraction (SAED) patterns shown in Figure S2 (Supporting information), as more diffuse rings can be seen with increasing DDA ratio. For all nanoparticles, the diffraction patterns can be indexed to hcp Ru.

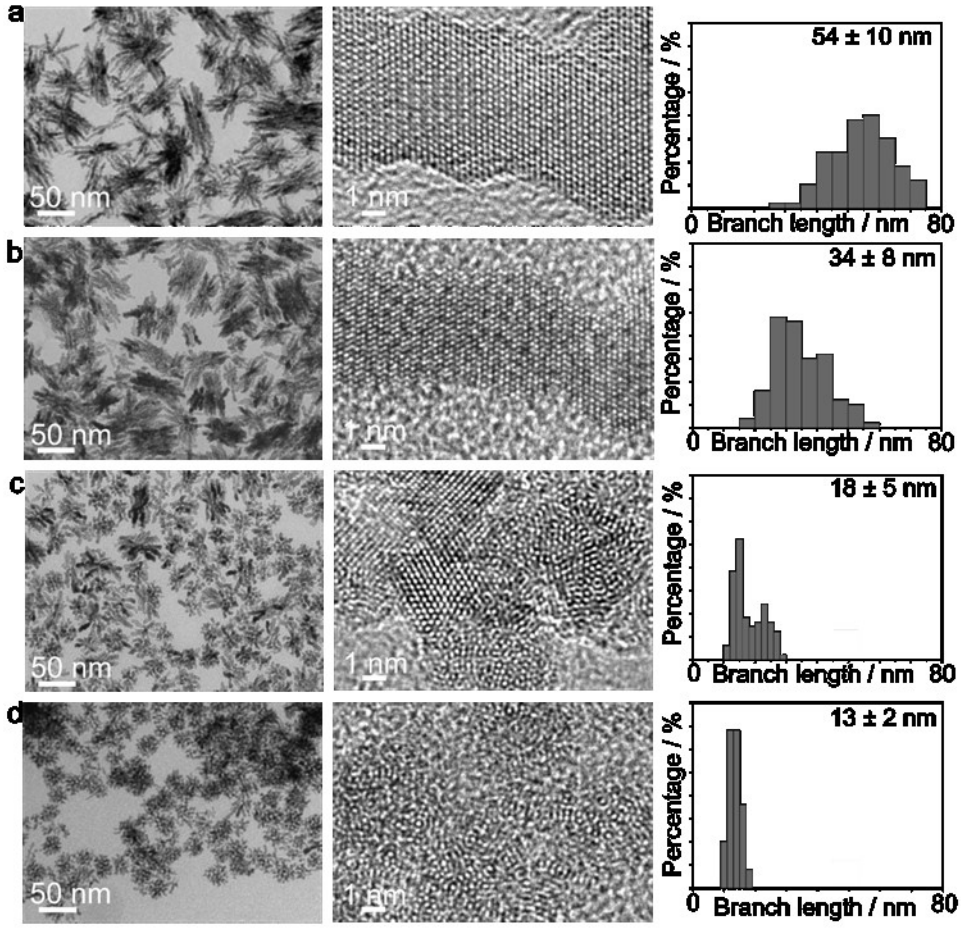

Figure 1. TEM images, HR-TEM images and corresponding size distributions of branched ruthenium nanoparticles with a) 5 mol equivalents b) 10 mol equivalents, c) 15 mol equivalents, and d) 20 mol equivalents dodecylamine surfactant.

These results show that the ratio of DDA relative to Ru controls the morphology and the crystallinity of the nanoparticles. Lower ratios of DDA produce branched nanoparticles with a single-crystalline structure (Figures 1a and b) while more than 10 mol equivalents of DDA prevents complete crystallization of branches (Figures 1c and

d). The lower ratio of DDA allows monomers in solution to readily access the branch surface to form surface facets.[7d,9] As the amount of dodecylamine surfactant is increased, the long-order of the Ru crystals is decreased and the crystallinity of Ru nanoparticles decreases to form polycrystalline nanocrystals. With higher ratios of surfactant above 10 mol equivalents, excess surfactant inhibits monomer addition and prevents further branch growth and crystallization.[10] The optimum ratio of DDA in this approach enables the formation of highly branched nanoparticles with single-crystalline structure.

Branched Ru nanoparticles that have been reported to date consist of aggregates of spherical polycrystalline Ru nanoparticles with no well-defined facets.[11] Aggregated Ru nanoparticles are formed with lower ratios (<1 mol equivalent) of polymer, amine or alcohol ligands by enabling rapid nucleation of Ru spheres and aggregation processes. Ru nanoparticles with well-defined surfaces have only been formed using 5 mol equivalents DDA, which allows monomer addition to create the low index facets on hourglass shaped nanoparticles.[9] To date, a simple synthetic method for controlling the crystallinity of Ru nanoparticles has not been reported, with post-synthesis annealing processes being commonly used instead.[12] It is important to readily tune the crystallinity in order to control the specific facets, defects and atomic arrangements at the surface of a nanoparticle, which are critical for catalysis.[12, 13] We show that changing the ratio of surfactant is a simple method to control the crystallinity of nanoparticles that can be applied to other one-pot or multi-step syntheses.

Detailed analysis of the surface facets of the branches by aberration-corrected high-resolution TEM (HRTEM) is shown in **Figure 2**. The nanoparticles synthesized with the lowest ratio of DDA (5 mol equivalents, Figure 1a) have angular branches that are indicative of faceted surfaces (Figure 2a). The branches are single crystalline, with a regular hcp structure that extends along the c-axis (Figure 2b), as shown by the fast Fourier transform (FFT) analysis of the image that matches a hcp crystal structure viewed down the <01-10> zone axis (Figure 2b, inset). The surface of the branches can be indexed to a mixture of {0001}, {10-11} and {10-10} facets with several defects along the edges. These defects are atomic steps made of n(10-11) x n(10-11) and edge atoms at n(10-11)xn(10-10) and n(10-11)xn(0001) that are higher in energy than the low index facets, but lower in energy than polycrystalline surfaces.[14] The interplanar separation of the {0002} planes is 0.21 nm which matches metallic Ru (Figure 2b). In contrast, a polycrystalline structure with rounded branch surfaces is formed with the highest ratio of DDA (20 mol equivalents , Figure 1d), without any surface faceting (Figure 2c) and unaligned crystalline regions of atoms (Figure 2d) as confirmed by FFT analysis of the image (Figure 2d, inset). By synthesizing branched Ru nanoparticles using low ratios of DDA, we achieve both highly branched and highly faceted nanoparticles which are important for achieving high surface area and enhanced electrocatalytic performance.

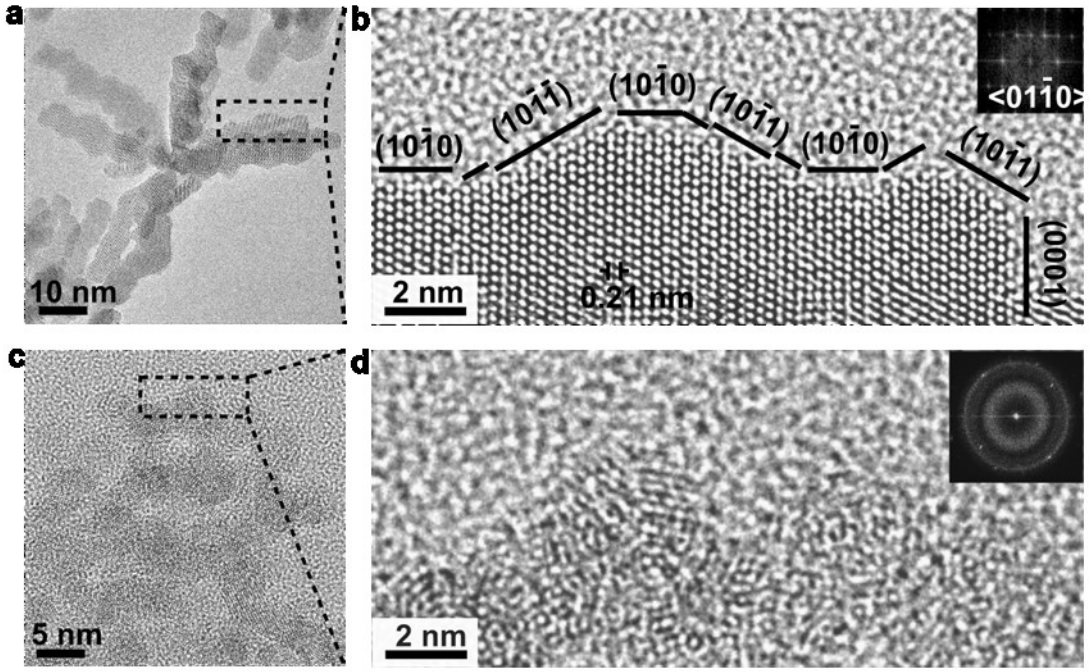

Figure. 2 a) TEM image of an individual branched nanoparticle synthesized with 5 mol equivalents of dodecylamine, from the sample shown in Figure 1a. b) HRTEM image of a branch indicated by the black box in (a) and the corresponding FFT (inset). The atoms are arranged in a hcp crystal structure viewed down the <01-10> zone axis. c) TEM image of an individual branched nanoparticle synthesized with 20 mol equivalents dodecylamine, from the sample shown in Figure 1d. d) HRTEM image of a branch indicated by the black box in (c) and the corresponding FFT (inset).

By comparing the faceted Ru branched and polycrystalline Ru nanoparticles in the OER electrocatalytic studies in acid electrolyte, we show that the faceted Ru branched nanoparticles are both more active and stable than polycrystalline Ru nanoparticles. The surface dodecylamine ligands are electrochemically removed by cycling several times between 1.10 and 1.45 V. This is shown by an increase in the

current density during the first few cycles as more catalyst surface is exposed to the electrolyte. A maximum current density is reached at cycle 4 for the faceted Ru branched nanoparticles and cycle 5 for polycrystalline Ru nanoparticles (Figure S3, Supporting information). The *i*R-corrected potentiodynamic curves (**Figure 3**a) show that, for the same mass of Ru, the faceted Ru branched nanoparticles reach a current density of 10 mA cm^{-2} at 1.41 V (vs the reversible hydrogen electrode - RHE) which corresponds to an overpotential of 180 mV. In comparison, the polycrystalline Ru nanoparticles only reach 4 mA cm^{-2} even when the potential is increased to 1.47 V.

The stability of nanoparticles was evaluated by chronopotentiometry at constant current of 10 mA cm^{-2}. [2c, 16] The faceted Ru branched nanoparticles are stable during OER over time, with the overpotential to produce 10 mA cm^{-2} current density increasing by only 85 mV after 4 hours, as shown in Figure 3b. Post-catalysis TEM characterization shows that facets are present after 4 hours stability testing (Figure S4, Supporting information), which confirms that the structure is stable. In contrast, the polycrystalline Ru nanoparticles are highly unstable and become completely inactive in less than 1 minute under the same applied current density.

The change in overpotential required to keep 10 mA cm^{-2} over time for the faceted Ru branched nanoparticles follows the same trend as the amount of dissolved Ru in the electrolyte measured by inductively coupled plasma mass spectrometry (ICP-MS), as shown by increase of the curves over time in Figure S5, Supporting information. The stability of the faceted Ru branched nanoparticles is due to the low

rate of dissolution of soluble oxidized species ($Ru^{>4+}$) that form under OER conditions,[4] with only 3 μg of Ru dissolved from the electrode after 60 minutes. For polycrystalline Ru nanoparticles, 22.26 μg Ru was dissolved into the electrolyte after 1 minute, which indicates that deactivation is caused by the complete dissolution of the nanoparticles.

The high stability of faceted Ru branched nanoparticles is also shown by the low Tafel slope of 52 mV dec^{-1} (Figure 3c) which is characteristic of stable OER catalysts[6,1b] where the rearrangement of the bonded -OH species prior to the second electron transfer is the rate-determining step.[17] The Tafel slope is the same after chronopotentiometry test (Figure S6, Supporting information). All Tafel slopes were analyzed in the range of potential where OER occurs to achieve 10 mA cm^{-2}. In contrast, unstable Ru nanoparticles typically show a Tafel slope >100 mV dec^{-1} with the first electron transfer as the rate-determining step.[17] A Tafel slope for the polycrystalline Ru nanoparticles could not be plotted due to their instability.[7b]

The faradaic efficiency (FE) for OER of faceted Ru branched nanoparticles is 99.6 % which is ~7x higher than the polycrystalline Ru nanoparticles (14.6 %), as shown in Figure 3d. These results show that faceted Ru branched nanoparticles are highly efficient OER catalysts for O_2 generation with only 0.4 % of the total charge resulting from oxidation of Ru, while for the polycrystalline nanoparticles, most of the charge (85.4 %) is generated from oxidation of Ru. The high stability against dissolution of faceted Ru branched nanoparticles results in 5x higher specific activity

than polycrystalline Ru nanoparticles (Figure 3d). The detailed calculations of FE and specific activity are available in the Supporting Information (Figure S7-8).

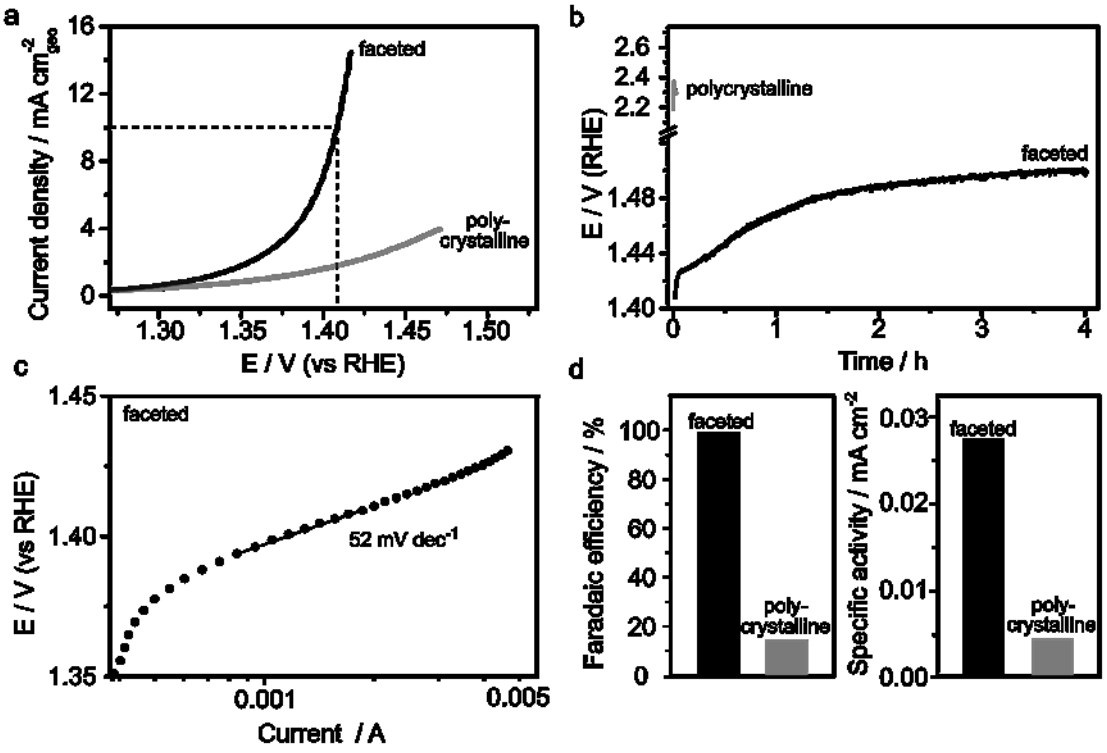

Figure 3. a) Potentiodynamic curves of OER performance for faceted Ru branched nanoparticles (black) and polycrystalline Ru nanoparticles (gray), obtained with scan rate 50 mV s^{-1} in 0.1 M $HClO_4$ at room temperature. b) Chronopotentiometric (CP) profile for faceted Ru branched nanoparticles (black) and polycrystalline Ru nanoparticles (gray) in 0.1 M $HClO_4$ at 1600 rpm. c) Tafel plot of faceted Ru branched nanoparticles with scan rate 50 mV s^{-1} in 0.1 M $HClO_4$. d) Faradaic efficiency and specific activity of the faceted Ru branched (black) and polycrystalline Ru (gray) nanoparticles.

The scheme in **Figure 4** illustrates the process occurring at branch surfaces during catalysis. Oxidized surface atoms either can catalyze OER or dissolve into acidic electrolyte under OER conditions. Ru atoms on faceted Ru branches are more stable against dissolution and so are available for OER catalysis, while only edge atoms, which are high energy sites, are more likely to be dissolved into solution (Figure 4a). Our work illustrates that low index facets provide much slower dissolution rates, the low index facets have fewer high energy defect sites at the surface leading to increased stability. This is supported by previous studies that show that lower energy surfaces are more stable in during OER.[6] For the polycrystalline Ru branches, most Ru atoms are at unstable low coordination sites that readily oxidized, resulting in completely dissolution of the catalyst (Figure 4b). The larger number of active surface atoms that remain at the surface of faceted Ru branched nanoparticles results in a five-fold improvement in activity and higher stability relative to polycrystalline Ru branched nanoparticles.

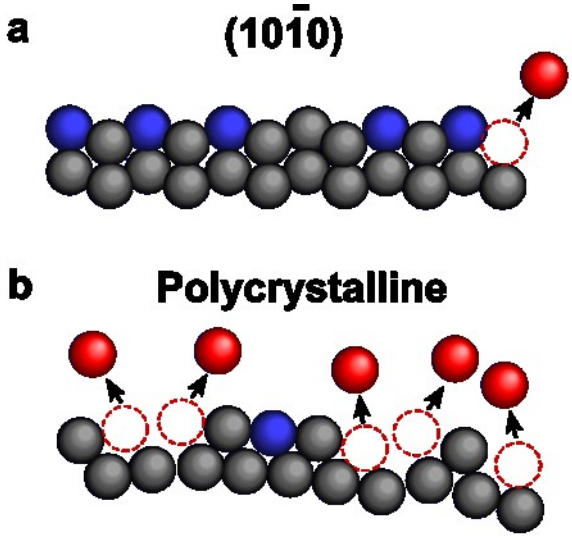

Figure 4. Scheme of the proposed structural changes affecting OER activity and stability of a) faceted Ru branched nanoparticles and b) polycrystalline Ru nanopartides. Blue atoms represent oxidized Ru sites where OER catalysis occurs. Red atoms represent oxidized Ru species that have dissolved from surface.

The overpotential at 10 mA cm^{-2} of faceted Ru branched nanoparticles is 240 mV lower than the state-of-art RuO_2.[7a] Unlike other Ru nanoparticle catalysts that completely dissolve in a few cycles,[7b, 18] faceted Ru branched nanoparticles are stable and active even after several hours under constant current density of 10 mA cm^{-2}. Ru{0001} films have been shown to be more stable compared to polycrystalline Ru due to their resistance to oxidation and dissolution.[19] The faceted branched Ru nanoparticles are stable due to low index facets, which results in an improvement in stability without compromising the activity. The Ru branched nanoparticles are the

first catalyst that achieve overpotential less than 300 mV after 2 hours stability test as compared to recent Ru and Ir nanoparticles based OER catalysts (Table S1, Supporting information). This can be achieved because of the low dissolution rate and resulting high Faradaic efficiency.

In conclusion, we have found that using low ratios of surfactant in the synthesis of branched Ru nanoparticles is key to achieving long, highly crystalline branches with low index facets. The use of strongly binding DDA surfactant enabled the formation of faceted surfaces on the branched nanoparticles. By achieving record-high stability and high activity for OER, we show that branching and faceting are key structural features for high performance nanocatalysts. The branched facets provided very high stability against Ru dissolution under OER conditions in an acid electrolyte, resulting in superior activity and stability for OER electrocatalysis. This work highlights the importance of synthetically controlling nanoparticle crystallinity to optimize surface properties for OER. Further, these results show the opportunity to control the crystallinity and surface structure of nanoparticles to improve activity and stability for electrocatalysis. These principles can be applied to a range of different metal nanoparticles, which will allow nanocatalysts to be created with high activity and stability that is needed for effective catalyst materials.

Experimental Section

Synthesis of branched ruthenium nanopartides: In a typical experiment, 0.1 mmol ruthenium (III) acetylacetonate (97%, Sigma Aldrich) and dodecylamine (98%, Sigma Aldrich)

dissolved in 2.0 mL 1-octadecene (90%, Sigma Aldrich). The solution was transferred into a Fischer-Porter bottle, which was evacuated and filled with 3 bar H_2 and sealed. The bottle was then placed in oil bath at 145°C for 48 hours. The resulting nanoparticles were purified by precipitation using a 1:1 v/v mixture of toluene and ethanol centrifugation at 3500 rpm for 5 minutes. The purification steps were repeated twice before storing the solid was in toluene. The product from each batch is approximately 7 mg of Ru nanoparticles with a 70% yield. When the amount of reaction mixture is doubled, the product is increased by 2x and the yield remains at 70%, which shows the possibility to scale up this synthesis.

Characterization: Transmission electron microscope (TEM) samples were prepared by drop-casting a solution of nanopartides suspended in cyclohexane onto a carbon coated copper grid or a grid containing a 10 nm thick SiN window. Low resolution TEM (LR-TEM) and high-resolution TEM (HR-TEM) images were taken on FEI Tecnai G2 20 TEM and JEOL JEM-F200 operating at 200 keV and FEI Titan ETEM with Image C_s corrector operating at 300 keV, respectively. The branch length is the length of the longest branch measured from the central branching point from at least 200 nanoparticles using ImageJ software.

Electrochemical measurements: The electrochemical measurements were conducted in a three-electrode system using N_2 saturated $HClO_4$ 0.1 M as the electrolyte with Pt mesh as counter electrode and Ag|AgCl|NaCl 3 M as reference electrode. In a typical experiment, 2.5 mg Ru nanoparticle sample were dispersed in 1 mL toluene and 10 µL of the solution was carefully dropped on a glassy carbon surface (0.196 cm^2) as the working electrode. The electrochemically active surface areas (ECSA) were determined from the double layer capacitance (C_{DL}) obtained by cyclic voltammetry.[20] The currents in the non-faradaic region (0.2 V) at different scan rates 10 mV s^{-1}, 25

mV s^{-1}, 50 mV s^{-1}, 75 mV s^{-1} and 100 mV s^{-1} were plotted against the scan rates to obtain the capacitances that were further used to calculate the ECSA by using the 66 µF cm^{-2} specific capacitance value.[21] The OER polarization curves were obtained by cyclic voltammetry at 50 mV s^{-1}. Stability was measured by chronopotentiometry at constant current of 10 mA cm^{-2} with the working electrode rotating at 1600 rpm. During the constant current experiments, the electrolyte was replaced every 10 minutes and analyzed by ICP-MS to calculate the Ru dissolution and account for the contribution of Ru dissolution to the total oxidation current.

Supporting Information

Supporting Information is available from the Wiley Online Library or from the author.

Acknowledgements

A.R.P., J.J.G. and R.D.T. gratefully acknowledge the University of New South Wales for the research funding. A.R.P. is currently a PhD candidate at School of Chemistry and is supported by an Australian Government Research Training Program Scholarship and the UNSW Scientia PhD Scholarship Scheme. L.G., J.J.G and R.D.T acknowledge funding under the Australian Research Council Linkage grant (LP150101014). Support from the Australian Research Council through the award of an Australian Laureate Fellowship (FT150100060) for J.J.G and a Discovery Project (DP190102659) for R.D.T. This research used the facilities supported by Microscopy Australia (formerly AMMRF) at the Electron Microscope Unit at UNSW. This work was performed, in part, at the Center for Integrated Nanotechnologies, an Office of Science User Facility operated for the U.S. Department of Energy (DOE) Office of Science. Sandia National Laboratories is a multimission laboratory managed and operated by National Technology and Engineering Solutions of Sandia, LLC., a wholly owned

subsidiary of Honeywell International, Inc., for the U.S. Department of Energy's National Nuclear Security Administration under contract DE-NA-0003525. This paper describes objective technical results and analysis. Any subjective views or opinions that might be expressed in the paper do not necessarily represent the views of the U.S. Department of Energy or the United States Government.

Received: ((will be filled in by the editorial staff))
Revised: ((will be filled in by the editorial staff))
Published online: ((will be filled in by the editorial staff))

References

[1] a) B. Lim, Y. Xia, *Angew. Chem.* **2011**, *123*, 78-87; *Angew. Chem. Int. Ed.* **2011**, *50*, 76-85; b) L. Gloag, T. Benedetti, S. Cheong, Y. Li, X.-H. Chan, L.-M. Lacroix, S. Chang, R. Arenal, I. Florea, H. Barron, A. Barnard, A. Henning, C. Zhao, W. Schuhmann, J. J. Gooding, R. D. Tilley, *Angew. Chem.* **2018**, *130*, 10398-10402; *Angew. Chem. Int. Ed.* **2018**, *57*, 10241-10245; c) L. Gloag, T.

M. Benedetti, S. Cheong, C. E. Marjo, J. J. Gooding, R. D. Tilley, *J. Am. Chem. Soc.* **2018**, *140*, 12760-12764.

[2] a) I. Man, H.-Y. Su, F. Calle-Vallejo, H. Hansen, A. Hansen, J. Martínez, Nilay, G. Inoglu, J. Kitchin, T. F Jaramillo, J. K Nørskov, J. Rossmeisl, *ChemCatChem* **2011**, *3*, 1159; b) H. Hwang, T. Kwon, H. Y. Kim, J. Park, A. Oh, B. Kim, H. Baik, S. H. Joo, K. Lee, *Small* **2018**, *14*, 1702353; c) C. C. L. McCrory, S. Jung, I. M. Ferrer, S. M. Chatman, J. C. Peters, T. F. Jaramillo, *J. Am. Chem. Soc.* **2015**, *137*, 4347-4357.

[3] Carmo, M.; Fritz, D. L.; Mergel, J.; Stolten, D., *Int. J. Hydrog. Energy* **2013,** *38*, 4901-4934.

[4] Danilovic, R. Subbaraman, K.-C. Chang, S. H. Chang, Y. J. Kang, J. Snyder, A. P. Paulikas, D. Strmcnik, Y.-T. Kim, D. Myers, V. R. Stamenkovic, N. M. Markovic, *J. Phys. Chem. Lett.* **2014**, *5*, 2474-2478.

[5] T. Reier, H. N. Nong, D. Teschner, R. Schlögl, P. Strasser, *Adv. Energy Mat*. **2017**, *7*, 1601275.

[6] S. H. Chang, N. Danilovic, K.-C. Chang, R. Subbaraman, A. P. Paulikas, D. D. Fong, M. J. Highland, P. M. Baldo, V. R. Stamenkovic, J. W. Freeland, J. A. Eastman, N. M. Markovic, *Nat. Commun.* **2014**, *5*, 4191.

[7] a) Y. Lee, J. Suntivich, K. J. May, E. E. Perry, Y. Shao-Horn, *J. Phys. Chem. Lett.* **2012**, *3*, 399-404; b) T. Reier, M. Oezaslan, P. Strasser, *ACS Catal.* **2012**, *2*, 1765-1772; c) E. A. Paoli, F. Masini, R. Frydendal, D. Deiana, C. Schlaup, M. Malizia, T. W. Hansen, S. Horch, I. E. L. Stephens, J. Chorkendorff, *Chem. Sci.* **2015**, *6*, 190-196; d) P. Lignier, R. Bellabarba, R. P. Tooze, Z. Su, P. Landon, H. Ménard, W. Zhou, *Crys. Growth Des.* **2012**, *12*, 939-942; e) L.

Gloag, T. M. Benedetti, S. Cheong, R. F. Webster, C. E. Marjo, J. J. Gooding, R. D. Tilley, *Nanoscale* **2018**, *10*, 15173 – 15177.

[8] L. Patricia, P. Karine, C. Bruno, *ChemCatChem* **2013**, *5*, 28-45.

[9] J. Watt, C. Yu, S. L. Y. Chang, S. Cheong, R. D. Tilley, *J. Am. Chem. Soc.* **2013**, *135*, 606-609.

[10] D. Li, S. Komarneni, *J. Am. Ceram. Soc.* **2006**, *89*, 1510-1517.

[11] Pelzer, K. , Vidoni, O. , Philippot, K. , Chaudret, B. and Collière, V, *Adv. Funct. Mater.* **2003**, *13*, 118-126.

[12] Y. Li, L. A. Zhang, Y. Qin, F. Chu, Y. Kong, Y. Tao, Y. Li, Y. Bu, D. Ding, M. Liu, *ACS Catal.* **2018**, *8*, 5714-5720.

[13] a) H. Petrova, J. Perez-Juste, Z. Zhang, J. Zhang, T. Kosel, G. V. Hartland, *J. Mater. Chem.* **2006,** *16*, 3957-3963; b) Q. Zhang, J. Xie, Y. Yu, J. Yang, J. Y. Lee, *Small* **2010,** *6* , 523-527.

[14] a) B. Lang, R. W. Joyner, G. A. Somorjai, *Surf. Sci.* **1972**, *30*, 440-453; b) W. P. Griffith, *Platinum Metals Rev.* **2009**, *53*, 209-215.

[15] a) E. J. Popczun, C. W. Roske, C. G. Read, J. C. Crompton, J. M. McEnaney, J. F. Callejas, N. S. Lewis, R. E. Schaak, *J. Mater. Chem. A* **2015**, *3*, 5420-5425; J. Watt, S. Cheong, M. F. Toney, B. Ingham, J. Cookson, P. T. Bishop, R. D. Tilley, *ACS Nano* **2010**, *4*, 396-402.

[16] Y. Wang, D. Yan, S. El Hankari, Y. Zou, S. Wang, *Adv. Sci.* **2018**, *5*, 1800064.

[17] L. A. De Faria, J. F. C. Boodts, S. Trasatti, *J. Appl. Electrochem.* **1996**, *26*, 1195-1199.

[18] S. Cherevko, S. Geiger, O. Kasian, N. Kulyk, J.-P. Grote, A. Savan, B. R. Shrestha, S. Merzlikin, B. Breitbach, A. Ludwig, K. J. J. Mayrhofer, *Catal. Today* **2016,** *262*, 170-180.

[19] J. X. Wang, N. S. Marinković, H. Zajonz, B. M. Ocko, R. R. Adžić, *J. Phys. Chem. B* **2001**, *105*, 2809-2814.

[20] C. C. L. McCrory, S. Jung, J. C. Peters, T. F. Jaramillo, *J. Am. Chem. Soc.* **2013**, *135*, 16977-16987.

[21] C. L. Green, A. Kucernak, *J. Phys. Chem. B* **2002**, *106*, 1036-1047.

Controlling the crystallinity of branched ruthenium nanoparticles shows improved electrocatalytic performance than the state-of-the-art ruthenium-based catalyst. Faceted ruthenium (Ru) branched nanoparticles are five times more active and more stable than polycrystalline Ru nanoparticles for oxygen evolution reaction in acid. The strategy to use highly crystalline nanoparticles with low index facets provides a platform for the further electrocatalyst development.

Keywords: nanoparticle, electrocatalysis, oxygen evolution, crystallinity, ruthenium

Agus R. Poerwoprajitno, Lucy Gloag, Tania M. Benedetti, Soshan Cheong, John Watt, Dale L. Huber, J. Justin Gooding, and Richard D. Tilley*

Formation of Branched Ruthenium Nanoparticles for Improved Electrocatalysis of Oxygen Evolution Reaction